Evaluation of the Sequential Behavior of Tieback Wall in Sand by Small Scale Model Tests

Seo, Dong-Hee*1 Chang, Buhm-Soo*2
Jeong, Sang-Seom*3 Kim, Soo-Il*4

요 지

본 연구에서는 사질토 지반에서의 굴착단계별 연성 벽체의 거동분석을 수행하기 위해 흙막이벽의 모형실험을 실시하였다. 모형 흙막이벽 실험에서는 재료의 역학적 특성이 비교적 널리 알려진 주문진 표준사를 이용하여 상대밀도가 79%, 41%, 24%인 모형지반을 조성한 후 모형벽체의 연성지수를 변화시켜 각 굴착단계별로 배면지반과 연성 벽체의 거동특성을 규명하였다.

본 연구에서는 벽체의 수평변위, 벽체의 배면에 작용하는 수평토압, 굴착으로 인한 배면지반의 침하량 및 침하영향거리, 벽체에 작용하는 앵커의 하중, 그리고 벽체에 작용하는 휨모멘트와 축력에 대해 굴착단계에 따라 살펴보고 이를 토대로 지반과 벽체의 거동특성을 분석하였다.

Abstract

In this study, a total of 12 types of sequential model tests were conducted at the laboratory for small scale anchored walls. The sequential behavior for flexible wall embedded in sand was investigated by varying degrees of relative density of Joomoonjin sand and flexibility number of model wall.

The model tests were carried out in a 1000mm width, 1500mm length, and 1000mm high steel box. Load cells, pressure cells, displacement transducer and dial gauges were used to measure the anchor forces, lateral wall deflections, lateral earth pressures and vertical displacements of ground surface, respectively. Limited model tests were performed to examine the parameters for soil-wall interaction model and the formulation of analytical method was revised in order to predict the behavior of anchored wall in sand.

Based on the model tests and proposed analytical method, model simulations were performed and the predictions by the present approach were compared with measurements by the model tests and predictions by other commercial programs. It is shown that the prediction by the present

*1 Member, Graduate Student, Dept. of Civil Eng., Yonsei University
*2 Member, Manager(Ph. D), KISTEC
*3 Member, Associate Professor, Dept. of Civil Eng., Yonsei University
*4 Member, Professor, Dept. of Civil Eng., Yonsei University

approach simulates qualitatively well the general trend observed for model test.

Keywords : Anchored wall, Flexibility number, Joomoonjin sand, Relative density, Sequential behavior, Soil-wall interaction

1. Introduction

Since Coulomb and Rankine have started to examine the lateral earth pressure acting on the wall, much work has been done in the area of soil-structure interaction of rigid retaining walls ; much less work has been done on flexible walls, let alone sequential behavior on flexible walls. The sequential soil-wall behavior is complicate since many complex construction sequences, different soil conditions, initial conditions, and rigidities of wall and anchor are involved.

At present there are several methods available for predicting the sequential behavior of flexible walls. Although those methods make slightly different assumptions, they can generally be classified into two different types : beam-column method and finite element method. The beam-column method analyzes the wall as a beam divided into a number of discrete segments and solves the governing equation by the finite difference schemes. The analytical programs such as Wallap, Excad, Sunex and YS-excad are developed using the beam-column method. The finite element method analyzes the soil mass and the wall by using proper models for a soil-wall system and is developed primarily by Clough and Duncan(1971), Clough and Tsui(1974) etc. The prediction by finite element method is useful for finding the wall deflection including the settlement behind wall. However, it is difficult to prescribe appropriate stress-strain behavior of soil and determine the material parameters needed for the soil-structure interaction model. In this respect, the authors have proposed the beam-column approach for the sequential behavior of flexible walls through full scale measurements and case histories(Kim, 1995a ; 1996b) and compared the predicted deflections, moment and earth pressure profiles with measured ones. The proposed method simulated relatively well the general trend of the observed ones with construction sequences but there was some inaccuracy in magnitude. The possible reason for this is uncertainty of construction sequence, inaccurate soil properties and field measurements. The authors believed that restrictions associated with the present approach could be overcome to some extent by ascertaining the soil properties, geometric and loading conditions through model tests.

The main objective of the present work is to evaluate the sequential behavior of anchored wall by small scale model test and to enhance the quality of the prediction by the proposed method with various model tests.

2. Proposed Analytical Method

An anchored wall can be modelled as a beam resting on nonlinear soil spring supports. The wall is modelled as a beam with a bending stiffness EI. The governing differential equation for the response of the beam can be formulated from different stages for proper simulation of the

construction sequence as follows :

(1) Unsupported Excavation Stage

$$EI\frac{d^4y(x)}{dx^4} = q(x) - K_h y(x) \tag{1}$$

(2) Anchor Stressing Stage

$$EI\frac{d^4y(x)}{dx^4} = q(x) - \left[K_h + \frac{AE'}{LS}\cos\theta\right]y(x) = q(x) - Ky(x) \tag{2}$$

where EI is the flexural stiffness of the beam, y(x) is the beam deflection, q(x) is the earth pressure at zero deflection of the beam, K_h is the coefficient of subgrade reaction of soil, AE′ is the axial stiffness of anchor, L is the unbonded lengh of anchor, S is the anchor-installed spacing, θ is the anchor-installed angle and K is the combined stiffness by soil spring and anchor.

After a beam is divided into a number of discrete segments, the finite difference method is used to solve those equations related to each construction stage by applying the boundary conditions. Next, to solve the governing equation the earth pressure-displacement curves are formulated as experimental curves obtained by model tests. The experimental earth pressure-displacement curves which represent piecewise linear interpolation are composed of a series of straight lines joining five data points which are the active coefficient, the at-rest coefficient, the passive coefficient, the reference displacements for the full active and passive earth pressures. The subgrade reaction modulus of soil is then obtained by the slope of experimental earth pressure-displacement curves.

The construction sequence for the wall is modelled by dividing a series of unloading and reloading sequences into several stages on the basis of the excavation to the proper excavation level and then stressing the anchor to the final excavation. The elasto-plastic analyses are run to take into account the experimental earth pressure-displacement curves for subgrade reaction modulus through an iterative procedure. For each iteration, the beam displacements from the previous solution are used to enter the nonlinear earth pressure-displacement curves and solution procedures are repeated until two successive iterations obtain sets of displacements that agree with an user-specified closure tolerance at all nodal points.

3. Experimental Work

Reliable wall behavior is directly related to the experimental testing. Therefore a well defined testing program in the laboratory is an essential step and the key to a successful understanding of a real soil-structure interaction. So a series of carefully controlled model tests has been conducted.

3.1 Property Tests

In model tests, Joomoonjin sand was used in order to ensure the soil properties. The pertinent information regarding the physical properties of the soil is given in Table 1. Triaxial compression

tests were conducted to choose effective strength parameters as shown in Table 2. To measure the wall rigidity of acrylic plate, tensile tests were carried out according to ASTM D638 (1994), D638M(1993) using the equipment of Universal Test Machine(Instron Model 4206). Model wall and anchor used in this study were summarized in Table 3.

Table 1. Soil properties

Particle-Size Distribution		Soil-Property Values
Maximum Particle Diameter(mm)	D_{max}	0.850(No. 20)
Minimum Particle Diameter(mm)	D_{min}	0.075(No. 200)
Diameter corresponding to 10% Finer(mm)	D_{10}	0.41
Diameter corresponding to 60% Finer(mm)	D_{60}	0.48
Uniformity Coefficient	D_u	1.17
Coefficient of Gradation	D_c	1.23
Maximum Void Ratio	e_{max}	0.897
Minimum Void Ratio	e_{min}	0.628
Maximum Dry Unit Weight(t/m^3)	γ_{dmax} <ASTM D4253-93>	1.609
Minimum Dry Unit Weight(t/m^3)	γ_{dmin} <ASTM D4254-91>	1.382
Specific Gravity of Soil Solids	G_s <ASTM D854>	2.63
Moisture Content(%)	w	0.3
Unified Soil Classification System	<ASTM D2487>	SP

Table 2. Effective strength parameters

Soil	Avg. Unit Weight (t/m^3)	Avg. Relative Density (%)	Cohesion (t/m^3)	Friction Angle (°)
Loose Sand	1.431	24.4	0	32.3
Medium Sand	1.467	40.9	0	35.1
Dense Sand	1.556	79.2	0	38.7

Table 3. Material properties for model wall and anchor

Model Wall							
Type	Thickness (mm)	Cross Area (m^2)	E (t/m^2)	I (m^4)	EI ($t-m^2$)	$\rho = H^4/EI$ ($m^4/t \cdot m^2$)	Log ρ ($m^4/t \cdot m^2$)
W-1	1.77	1.18E-03	2.685E+05	0.461E-09	0.124E-03	6579.64	3.82
W-2	2.88	1.91E-03	2.724E+05	1.984E-09	0.540E-03	1507.11	3.18
W-3	3.98	2.64E-03	2.596E+05	5.238E-09	1.360E-03	599.01	2.78
W-4	4.95	3.29E-03	2.719E+05	10.118E-09	2.751E-03	296.06	2.47

Model Anchor		
Cross Area(mm^2)	Free Length(mm)	E ($t \cdot m^2$)
0.385	1040	9.47

3.2 Model Tests

The model tests were conducted in a 1000mm width, 1500mm length, and 1000mm high steel tank. A celluloid sheet was attached inside the sample container to reduce wall friction. Also, 10mm-high discrete panels were installed on the excavated side of model wall to simulate sequential excavation of sand deposits. Plan and sectional view of test devices are given in Fig. 1 and in Fig. 2, respectively.

Four test walls of acrylic plate, having thicknesses in the range of 1.77mm to 4.95mm, were built. The corresponding logarithm of flexibility number ρ(unit, $m^4/t \cdot m^2$) of these walls were in the range of 2.47 to 3.82. Here the flexibility number ρ is expressed as H^4/EI. Where H is the total height of wall drive, E is the modulus of elasticity of the wall material, and I is the moment of inertia of the wall section per unit length of the wall.

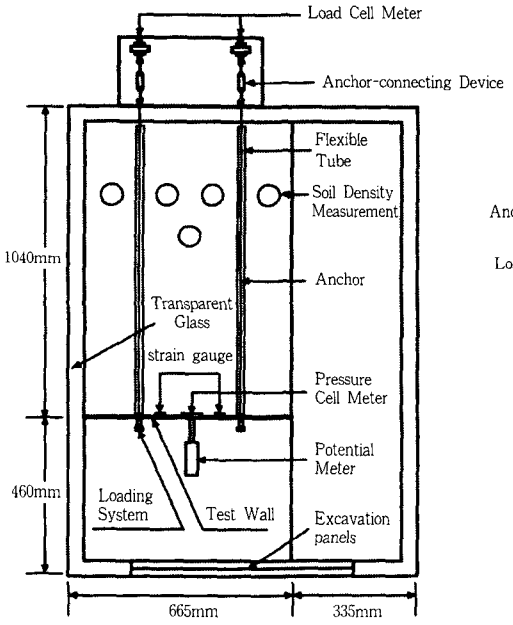

Fig.1 Plan view of test apparatus

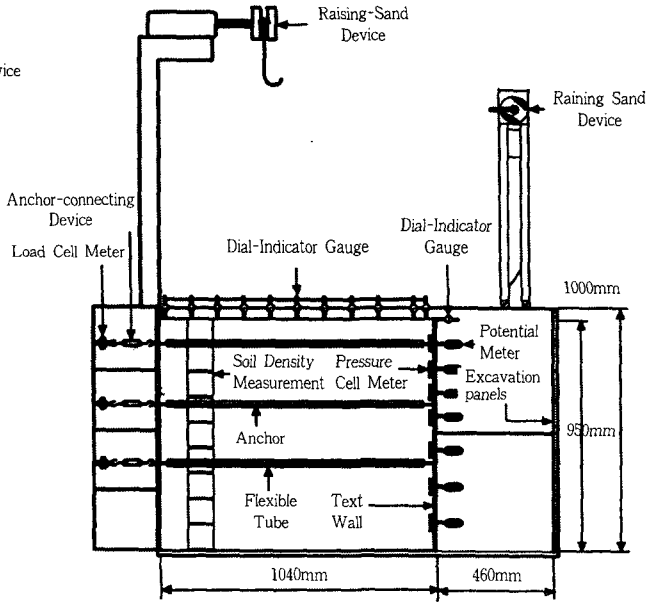

Fig.2 Sectional view of test apparatus

The magnitude of side friction and the dimensions of the wall necessary to reduce side friction effects to negligible proportions have been analyzed by Terzaghi, Arthur and Roscoe, Rowe, Bransby, etc(Bransby and Smith, 1975). Compared with these previous works, the width/height ratio of wall used in this study (0.7) was turned out to be beyond the range which the side friction becomes negligible. But about-1mm gap between the wall and the sides of the sample box is maintained to reduce side friction as much as possible and all measurements for the sequential behavior of soil-wall were performed on the central portion which is not affected by the side friction. Also, friction-reduced tapes were used to reduce the total quantity of soil friction at the wall-sample box interface and to maintain the uniform soil behavior in the sequential construction.

Through pre-tests, there are little difference in displacement and ground settlement between the central and the side parts of wall. This shows that all measured values do not have significant side friction effects. The anchor wires were made of high yield steel, threaded horizontally through polythene tubing in sand to eliminate the effects of friction between the wires and the sand.

Load cells, pressure cells, displacement transducer and dial gauges were used to measure the anchor forces, lateral wall deflections, lateral earth pressures and vertical displacements of ground surface respectively. Table 4 shows measuring units used in this study.

By varying wall flexibility and soil properties the total 12 types of sequential model tests were conducted. Test stages were determined by considering construction sequences of in situ structures and the detailed construction stages are in Table 5. According to literature review it was found that the factors that controlled the soil unit weight were the intensity of the soil raining, i.e. the weight deposited per unit area in unit time, and the height of fall of the particles. As shown in Fig. 3, raining-sand device which is capable of controlling regularly the intensity of raining and the height of particle fall was used. For a given height, an increase in the intensity increased the soil unit weight, while for a given intensity, an increase in the height of fall decreased the soil unit weight. In order to form the soil uniformly with depths, method to control the soil unit weight by the intensity of the fall was adopted in this study. And the gap-sizes of raining-sand device were determined through pre-tests (Table 6).

Table 4. Measuring units for instrumentation

Item	Instrument	EA	Measured Range	Sensitivity
Lateral Displacement of Wall	Potentialmeter	7	0.00~50.00mm	0.01mm
Lateral Earth Pressure	Pressure Cell	5	0.000~50.000kg/cm^2	0.001kg/cm^2
Anchor Load	Load Cell	6	0.00~100.00kg	0.01kg
Settlement of Ground Surface	Dial-Indicator Gauge	11	0.00~30.00mm	0.01mm
Bending Moment & Axial Force	Strain Gauge	22	0.00~10000.00μ	0.01μ

Table 5. Procedures of model test

Construction Sequences of Model Test	Position
Installation and Instrumentation	·
Sand-Deposition	·
Soil-Stabilization	·
Initial Measurement(Stage 0)	·
First Excavation(Stage 1)	About 17% of Final Excavation Depth
First-Anchor Installation and Stressing(Stage 2)	About 11% of Final Excavation Depth
Second Excavation(Stage 3)	About 44% of Final Excavation Depth
Second-Anchor Installation and Stressing(Stage 4)	About 39% of Final Excavation Depth
Third Excavation(Stage 5)	About 72% of Final Excavation Depth
Third-Anchor Installation and Stressing(Stage 6)	About 67% of Final Excavation Depth
Fourth Excavation(Stage 7)	About 89% of Final Excavation Depth
Fifth Excavation(Stage 8)	About 100% of Final Excavation Depth

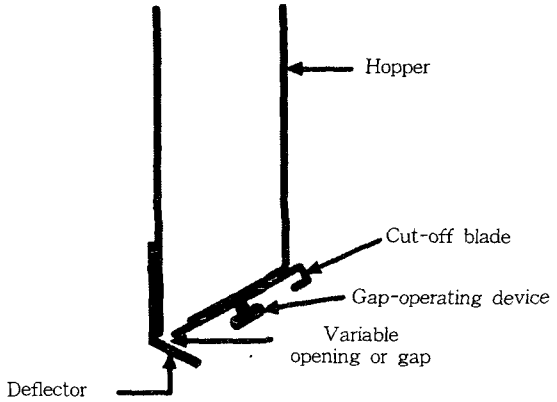

Fig. 3 Raining-Sand Device

Table 6. Model soil prepared by raining-sand Device

Gap Interval	2.00cm		0.88cm		0.36cm	
Soil Type	Loose		Medium		Dense	
Depth (cm)	Unit Weight (t/m^3)	Relative Density(%)	Unit Weight (t/m^3)	Relative Density(%)	Unit Weight (t/m^3)	Relative Density(%)
90~95	1.40	11.3	1.44	26.9	1.52	62.8
80~90	1.41	11.7	1.45	33.3	1.52	64.7
70~80	1.43	23.1	1.46	36.2	1.54	71.6
60~70	1.44	27.8	1.46	37.6	1.56	79.4
50~60	1.44	28.6	1.46	39.4	1.57	85.8
40~50	1.45	31.5	1.47	41.7	1.57	85.0
30~40	1.45	31.5	1.47	44.0	1.58	88.3
20~30	1.45	33.9	1.48	47.5	1.59	94.1
10~20	1.46	35.9	1.49	51.1	1.59	93.3
0~10	1.45	32.9	1.53	67.4	1.59	93.3
Avg.	1.43	24.4	1.47	40.9	1.56	79.2

4. Test Results

4.1 Sequential Lateral Displacements of Wall

Fig. 4 shows that as log ρ increases, δ_{Hmax}/H normalized by H_f varies in the range of 0.41% to 1.21% for 79%-Dr soil, 0.61% to 1.50% for 41%-Dr soil and 0.76% to 1.90% for 24%-Dr soil. Here, log ρ is flexibility number of wall, δ_{Hmax} is maximum lateral displacement of wall, H is the excavation depth, H_f is the final excavation depth, and Dr is the relative density of soil. It is also shown that δ_{Hmax}/H increases linearly until H/H_f approaches approximately to 72% whereas $\delta_{Hmax}/$

H does not vary excessively after reaching about 72%. As a result, δ_{Hmax} no longer varies, provided that H exceeds about 72% of H_f.

Next, Fig. 5(a) shows the relation of δ_{Hemax} and δ_{Hmax} as a function of H/H_f. Here δ_{Hemax} is the maximum lateral displacement of wall at each sequence. From this figure, $\delta_{Hemax}/\delta_{Hmax}$ on 79%-Dr and 41%-Dr soil is slightly larger than that of 24%-Dr soil. As a result, as Dr decreases, δ_{Hmax} increases but $\delta_{Hemax}/\delta_{Hmax}$ tends to decrease gradually.

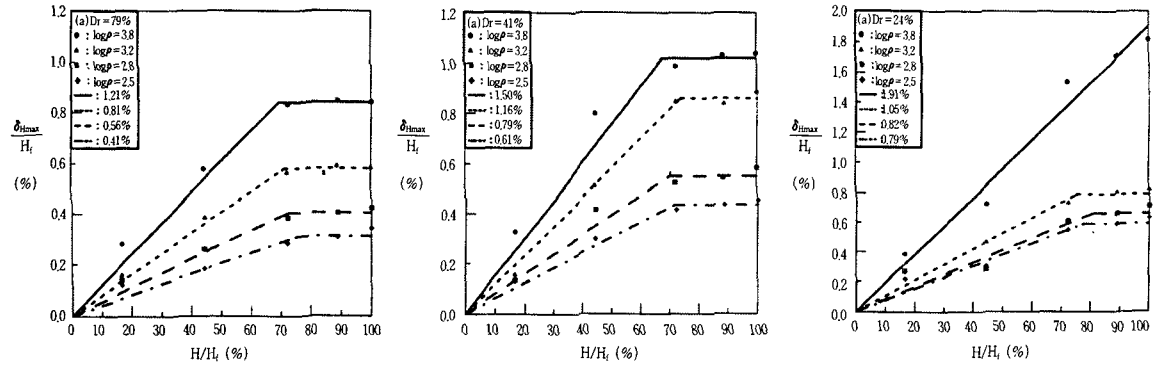

Fig. 4 Relation of H/H_f and δ_{Hmax}/H_f

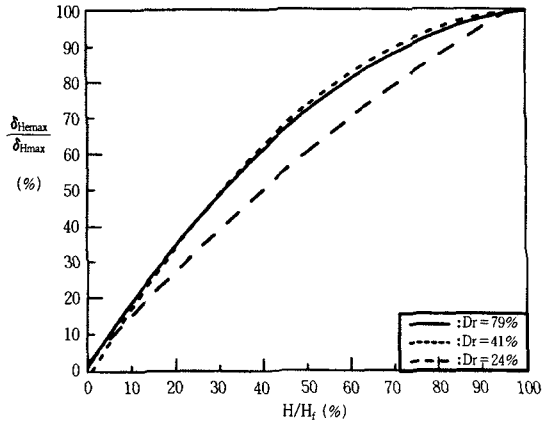

Fig. 5(a) Relation of H/H_f and $\delta_{Hemax}/\delta_{Hmax}$ with relative density

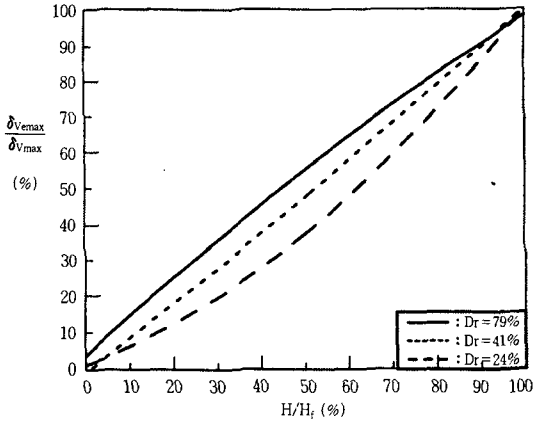

Fig. 5(b) Relation of H/H_f and $\delta_{Vemax}/\delta_{Vmax}$ with relative density

4.2 Sequential Ground Settlement

Fig. 6(a) shows that as H is about 17% of H_f, the influential distribution of ground surface settlement(D_I) is similar to 0.5 times of H_f suggested by Terzaghi and Peck(1967) on sand. Fig. 6(b) shows that as H is about 44% of H_f, the vertical displacements of ground surface(δ_V) is within the envelope of settlement suggested by Goldberg(Yang, 1996) on the wall which log ρ is

lower than 3.8. Also, in case of the wall which log ρ is 3.8, δ_V suggested by Peck is about 1.0%(1969) on sand. Based on the criterion of Apparent Influence Range(A.I.R) suggested by Ou (1993), most settlement was distributed within A.I.R. Fig. 6(c) shows that as Dr decreases and H gradually increases to H_f, the influential distribution of ground surface settlement on sand approaches up to 1.5 times H_f.

Next, the linear relation of δ_{Vmax} and H normalized by H_f is shown in Fig. 7. As log ρ increases δ_{Vmax} varies in the ranges of 0.36% to 1.06% times H for 79%-Dr soil, 0.73% to 1.97% times H for 41%-Dr soil and 0.94% to 2.40% times H for 24%-Dr soil. And the relationship between H $/H_f$ and $\delta_{Vemax}/\delta_{Vmax}$ is generalized as a second-degree regression curve as shown in Fig. 5(b). Here, δ_{Vemax} is maximum settlement of ground surface at each sequence. As a result, as Dr decreases, δ_{Vmax} increases but $\delta_{Vemax}/\delta_{Vmax}$ tends to increase gradually.

The characteristics between δ_{Hmax} and δ_{Vmax} normalized by H_f are analyzed as shown in Fig. 8. From this figure, it is found that $\delta_{Vmax}/\delta_{Hmax}$ varies in ranges of 0.8 to 1.7 on 79%-Dr soil, 0.8 to 1.9 on 41%-Dr soil and 0.8 to 2.0 on 24%-Dr soil. Comparing with the ranges of 0.5 to 1.0 on soft and medium-stiff clay suggested by Mana and Clough(1981), the ranges on sand by this model test are relatively large.

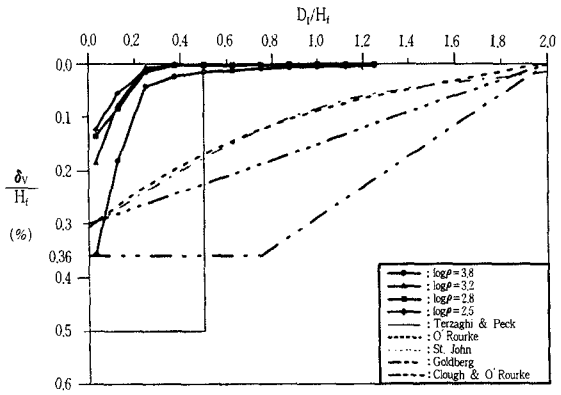

Fig. 6(a) Relation of D_I/H_f and δ_v/H_f
(Dr = 41%, H/H_f = 17%)

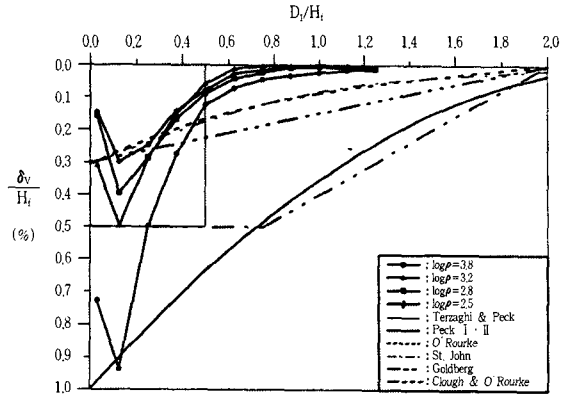

Fig. 6(b) Relation of D_I/H_f and δ_v/H_f
(Dr = 41%, H/H_f = 44%)

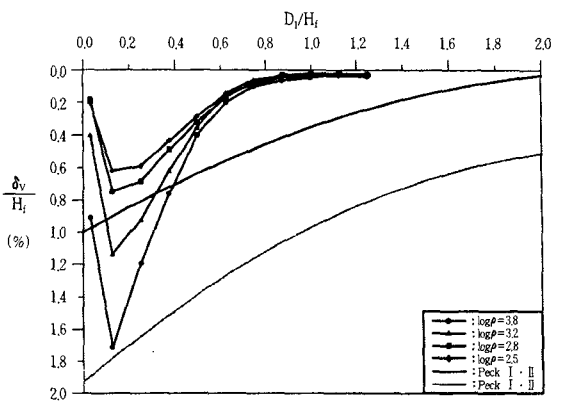

Fig. 6(c) Relation of D_I/H_f and δ_v/H_f
(Dr = 41%, H/H_f = 72%)

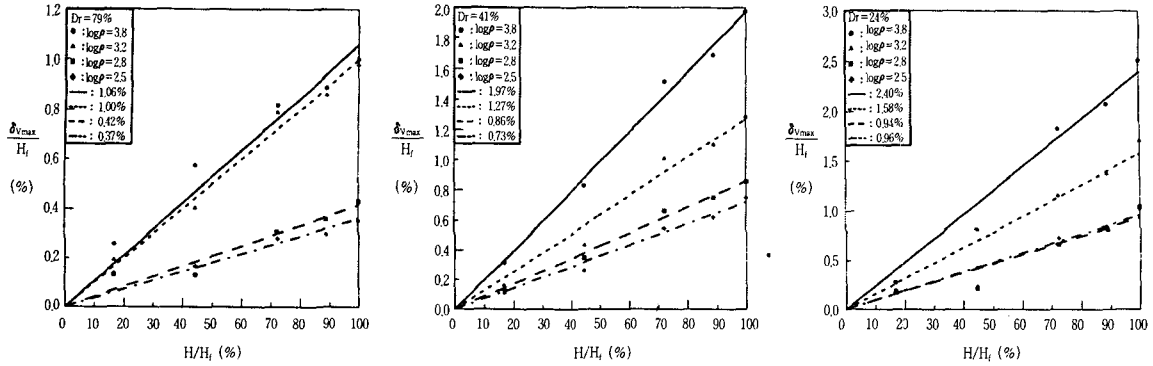

Fig. 7 Relation of H/H_f and δ_{Vmax}/H_f

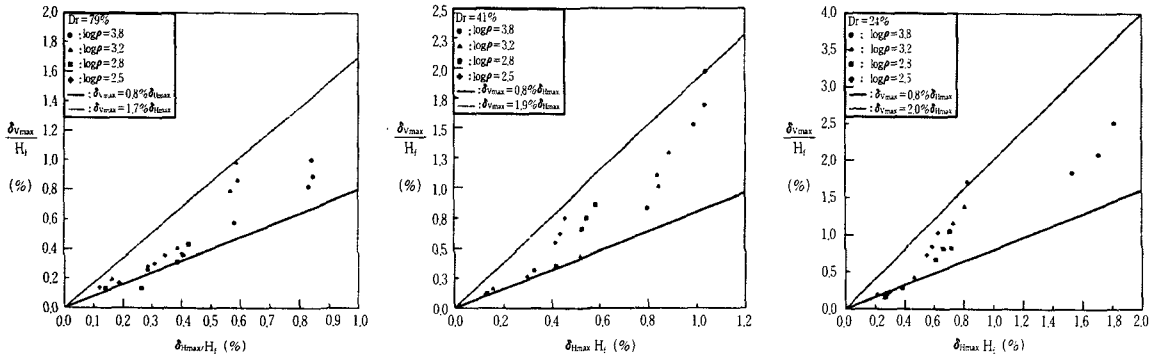

Fig. 8 Relation of δ_{Hmax} and δ_{Vmax} at final excavation depth

4.3 Sequential Distribution of Lateral Earth Pressure

Based on the model tests, the sequential distribution of lateral earth pressure acting on the wall was compared with empirical earth pressure envelopes on sand suggested by many researchers. Fig. 9(a) shows that as H is about 17% of H_f the distribution of lateral earth pressure is similar to that obtained from model tests on rigid wall by Fang and Ishibashi(1986). From this figure, it is found that on the wall deformation mode of rotating about wall bottom the general trend on the distribution of lateral earth pressure is quite similar irrespective of whatever wall is rigid or flexible.

The earth pressure acting on the moving part of the wall decreased and the earth pressure acting on the stable part of the wall increased at the stage of anchor-stressing. This phenomenon of pressure transfer is judged as arching effect(Terzaghi and Peck, 1967). Finally, Fig. 9(b) shows that as H increases the lateral earth pressure is distributed within the ranges of the envelope empirically suggested by Tschebotarioff and Schnabel(Kim, 1993). From this experiments, it is concluded that the empirical envelopes suggested by Tschebotarioff and Schnabel may be applied to design and analysis for deep-excavated anchored flexible wall.

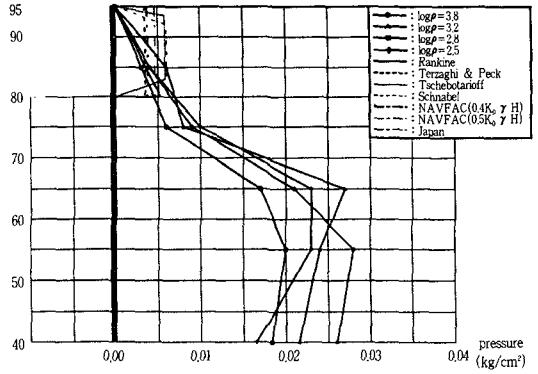

Fig. 9(a) Distribution of lateral earth pressure (Dr = 79%, H/H_f = 17%)

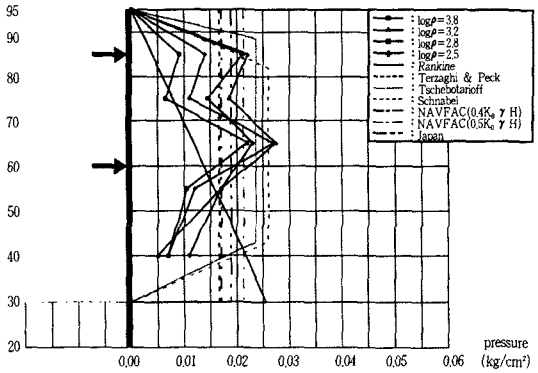

Fig. 9(b) Distribution of lateral earth pressure (Dr = 41%, H/H_f = 72%)

4.4 Sequential Variation of Anchor Load

In this study, the relation of anchor position and anchor force distributed by lateral earth pressure was analyzed according to sequential stages. The first row anchor was installed at about 11% of H_f, the second row anchor at about 39% of H_f, and the third row anchor at about 67% of H_f. Also, the initial anchor load was applied equally. Fig. 10 shows that the anchor force of first row on lateral earth pressure is almost constant though excavation depth increases. The force distribution of the second and third row anchor on lateral earth pressure does not vary for 79%-Dr soil whereas for 41% and 24%-D_r soil, there are gradual increases in the anchor force.

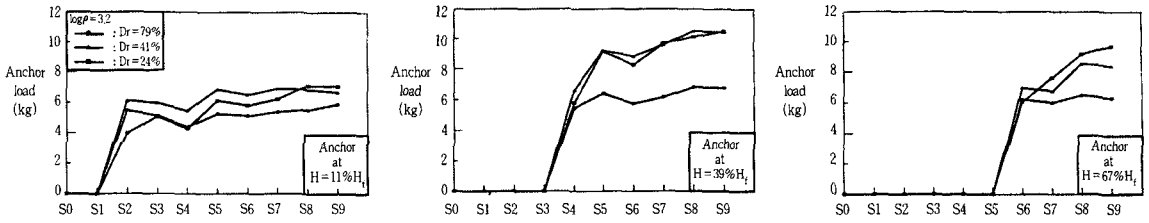

Fig. 10 Relation of anchor position and variation of anchor force

4.5 Sequential Variation of Bending Moment and Axial Force

A cubic spline function was used for the interpolation of the measured bending moment data which were commonly scattered. A cubic spline function is such that the interpolant is continuous and differentiable and that the first or second derivatives are continuous. As wall flexibility increases and relative density of soil decreases, bending moment acting on the wall is highly developed. Fig. 11 shows that the bending moment on the wall is highly influenced by the variation of wall flexibility, compared to the variation of relative density of soil. Fig. 12 shows that the variation of maximum bending moment is almost constant, provided that excavation depth exceeds

about 42% of wall height.

Fig. 13 shows that axial force is not developed nearly at bottom of the wall. And as excavation depth increases the axial force at the anchor-installed wall portion is developed a little more than that of the anchor-uninstalled wall portion.

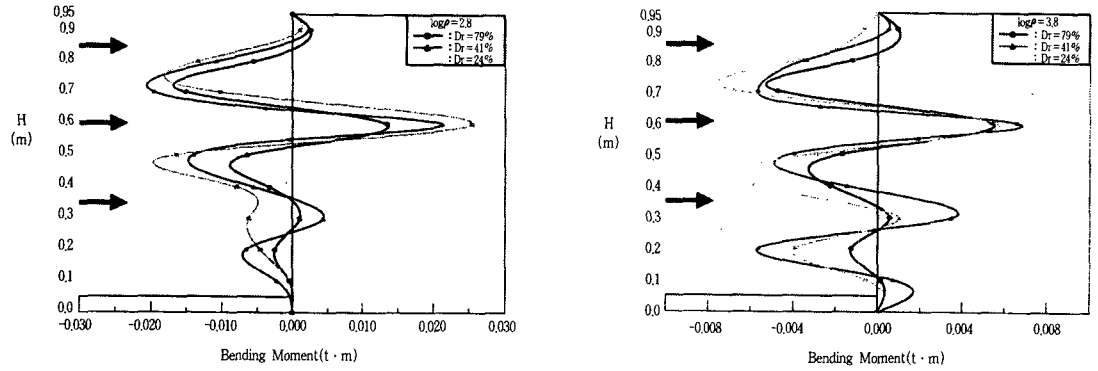

Fig. 11 Variation of bending moment($H = 100\%H_f$)

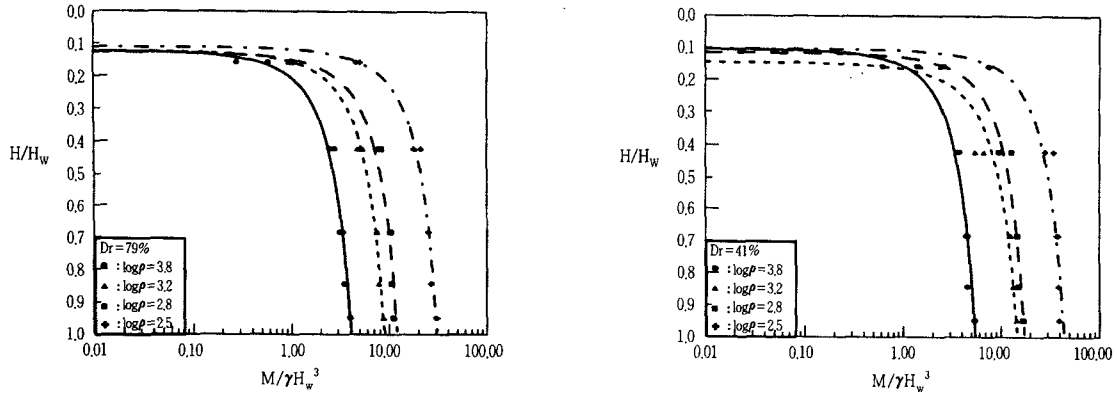

Fig. 12 Variation of bending moment with excavation depth

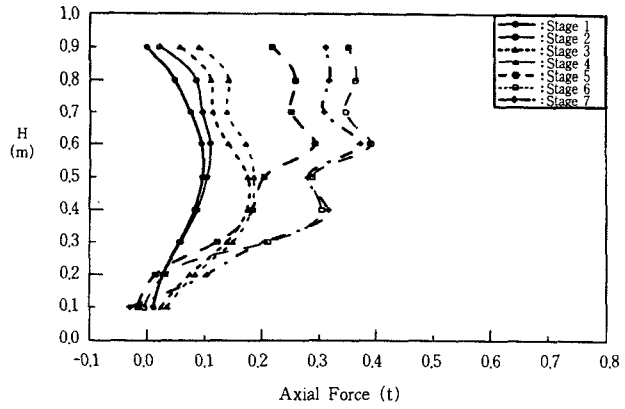

Fig. 13 Sequential variation of axial load($D_r = 79\%$, log e = 2.8)

4.6 Experimental Earth Pressure-Displacement Curve

The lateral earth pressure can be normalized by dividing the lateral earth pressure by the vertical effective stress at that depth. For a cantilevered excavation, the wall displacement occurred at a certain depth can be related to the normalized earth pressure at that depth. For an anchor-stressing construction stage, the wall moves back into the soil mass due to the anchor force. So model tests were carried out to experimentally get the relationship of lateral earth pressure and displacement. First in order to find the active coefficient and the reference displacement for the full active earth pressure, the active state test was performed that cantilevered excavation is proceeded continuously. Secondly in order to find the passive coefficient and the reference displacement for the full passive earth pressure, the passive state test was performed so that constant anchor force could be applied continuously. In a series of these procedures, the characteristic earth pressure-displacement curves are experimentally constructed and used in the revision of analytical formulation. As a result, Fig. 14 shows experimental earth pressure-displacement curves obtained by this study. Table 7 and 8 show the coefficient of limit earth pressure and the reference displacement ratio for the full active and passive earth pressure on anchored flexible wall embedded in sand.

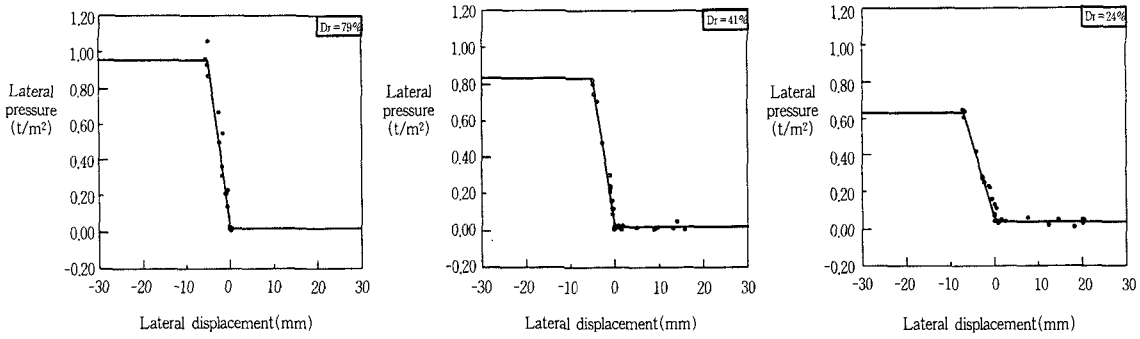

Fig. 14 Earth pressure-displacement curves based on model tests

Table 7 Coefficients of limit plastic earth pressure

Soil Type	Average Unit Weight	Avg. Dr.(%)	Limit Active	At-Rest	Limit Passive
			K_a	K_0	K_p
Dense	1.56	79	0.133	0.160	6.334
Medium	1.47	41	0.174	0.199	5.882
Loose	1.43	24	0.259	0.405	4.468

Table 8 Reference displacement ratio for the full active and passive earth pressures

Soil Type	Average Unit Weight	Avg. Dr.(%)	Friction Angle (°)	Cohesion (t/m^2)	y_a : y_p
Dense	1.56	79	32.3	0	1 : 5
Medium	1.47	41	35.1	0	1 : 4
Loose	1.43	24	38.7	0	1 : 5

5. Comparison of Observed Performance Based on Analytical Method

Based on the characteristics of the sequential behavior on flexible wall by model tests, the proposed approach, nonlinear soil-wall interaction model, is revised for the anchored flexible wall embedded in sand. Since the results of the proposed model are strongly influenced by the horizontal subgrade reaction modulus, the known values of movement required to reach the maximum passive and minimum active earth pressure were determined through on this model tests. For more detailed information of the analytical method, readers are referred to Chang(1998). Based on the model test and revised analytical method, model simulations were performed and the predictions were compared with the following cases.

Case 1

This case is model test that the Dr of soil is 79% and the log ρ is 3.8. In order to compare and analyze the revised analytical method with other commercial programs, the Crisp program of FEM code and the Sunex program using beam-column method for retaining wall were used on the same condition that the known data of model test were used for all input parameters. In this case, the sequential lateral displacement of wall is shown quantitatively as shown in Fig. 15(a). Fig. 16 (a) shows that the predicted lateral displacement is much similar to the observed one than the predicted one by other commercial programs.

Case 2

This case is model test that the Dr of soil is 41% and the log ρ is 2.5. In this case, the sequential lateral displacement of wall is shown quantitatively as Fig. 15(b). Also, Fig. 16(b) shows that the prediction by the present approach simulates well the general trend observed for model test.

Case 3

This case is model test that the Dr of soil is 24% and the log ρ is 2.5. In this case, the sequential lateral displacement of wall is shown quantitatively as Fig. 15(c). Fig. 16(c) shows the same result as case 1 and case 2.

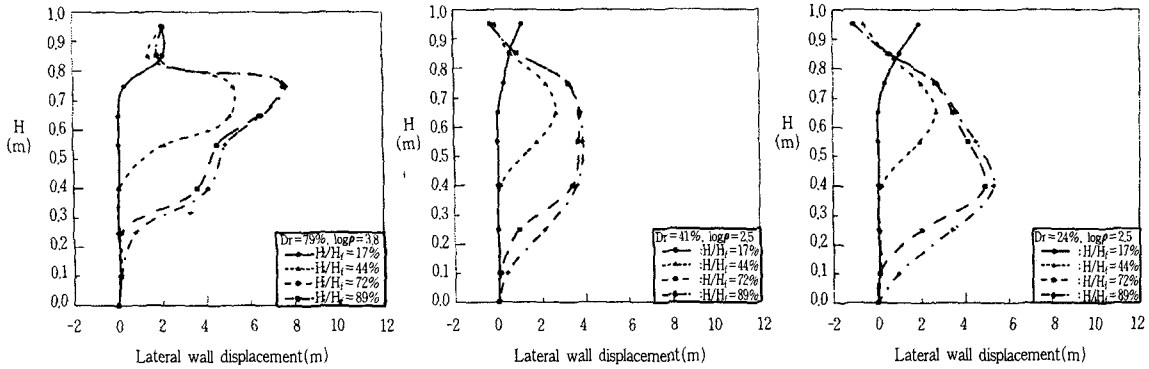

Fig. 15 Sequential lateral displacement of wall by model tests

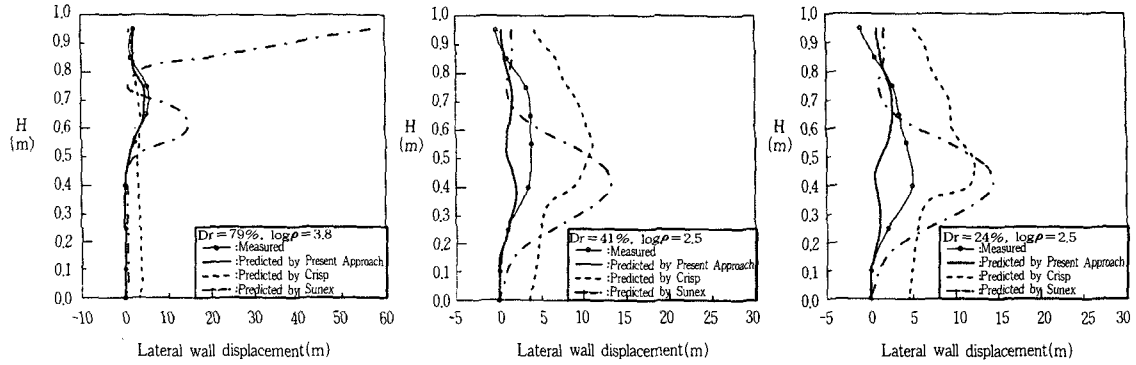

(a) case 1 (b) case 2 (c) case 3

Fig. 16 Comparison of deflection shape

6. Summary and Conclusions

In this study, the sequential behavior of flexible walls embedded in sand was investigated based on model tests and on an analytical study. Limited model tests were performed to examine the parameters for soil-wall interaction model and the formulation of analytical method was revised in order to predict the behavior of anchored wall in sand. And the prediction of present approach was compared with the test result. Based on this study, the following conclusions are drawn :

1) The maximum lateral displacement of wall(δ_{Hmax}) is no longer varied, provided that excavation depth(H) exceeds about 72% of final excavation depth(H_f). As the relative density of soil(Dr) decreases and H increases to H_f gradually, the influential distribution of ground surface settlement approaches up to 1.5 times H_f in case of anchored flexible wall in sand. Maximum settlement of ground surface(δ_{Vmax}) occurs in the ranges of 0.8 to 2.0 times δ_{Hmax} on the three different soil types.

2) As the relative density of soil(Dr) decreases, δ_{Hmax} increases but $\delta_{Hemax}/\delta_{Hmax}$ decreases gradually. While δ_{Vmax} increases $\delta_{Vemax}/\delta_{Vmax}$ increases gradually as Dr decreases. Here, δ_{Hemax} and

δ_{Vemax} are the maximum lateral displacement of wall and maximum settlement of ground surface at each sequence.

3) On the wall deformation mode of rotating about wall bottom the general trend on the distribution of lateral earth pressure is quite similar irrespective of whatever wall is rigid or flexible. As H increases the lateral earth pressure is distributed within the ranges of the envelope empirically suggested by Tschebotarioff and Schnabel.

4) The bending moment acting on the wall is highly influenced by the variation of wall flexibility, compared to the variation of relative density of soil. The variation of maximum bending moment is almost constant, provided that H exceeds about 42% of wall height.

5) On anchored flexible wall embedded in sand, the reference displacement ratio for the full active and passive earth pressures becomes approximately 1:4 to 1:5 which is not highly influenced by the variation of relative density.

6) The prediction by present approach simulates qualitatively well the general trend observed for model test.

Acknowledgement

This work in this paper was supported by grant No. 971-1201-002-2 from the Basic Research program of the KOSEF.

References

1. Annual Book of ASTM Standards D638(1994), D638M(1993), D854(1993), D2487(1993), D4253(1993), and D4254(1991), American Society for Testing and Materials, 1916 Race St., Philadelphia, PA 19103
2. Bransby, P. L., and Smith, Ian A. A.(1975), Side friction in model retaining-walls experiments, Proc, J. of the Geotech. Eng. Div., ASCE, Vol. 101, No. GT7, July, pp. 615-632
3. Chang, B. S.(1998), Back analysis of braced excavation using elastoplastic load-deformation characteristics of ground, Ph.D. Dissertation, Yonsei University
4. Clough, W. G., and Duncan, J. M.(1971), Finite element analyses of retaining wall behavior, J. of the Geotech. Eng., ASCE, Vol. 97, No. 12, pp. 1657-1673
5. Clough, W. G., and Tsui, Y.(1974), Performance of tieback walls in clay, Proc. J. Geotech. Div., ASCE, Vol. 12, No. 100, pp. 1259-1273
6. Fang, Y. S., and Ishibashi, I.(1986), Static earth pressures with various wall movements, J. of Geotech. Eng., ASCE, Vol. 112, No. 3, pp. 317-333
7. Kim, N. K., A beam-column method for tieback walls, Ph.D. Dissertation, Texas A&M University
8. Kim, S. I., Chang, B. S., and Jeong, S. S.(1995), Analysis of earth retaining structures by coupling of soil springs using p-y curves, Proc. of the 5th EASEC, pp. 1703-1708
9. Kim, S. I., Chang, B. S., Kim, H., and Jeong, S. S.(1996), Sequential analysis of earth retaining structures by using p-y curves for subgrade reaction, Proc. of the 3th Asian-Pacific Conference on Computational Mechanics, Vol. 3, pp. 2011-2016
10. Mana, A. I., and Clough, G. W.(1981), Prediction of movements for braced cuts in clay, J. of the Geotech. Eng. Div., ASCE, Vol. 107, No. GT6, pp. 759-777

11. Ou, C. Y., Hsieh, P. G., and Chiou, D. C.(1993), Characteristics of ground surface settlement during excavation, Canadian Geotechnical Journal, Vol. 30, pp. 758-767
12. Peck, R. B.(1969), Deep excavations and tunneling in soft ground, Proc. of 7th Inter. Conf. on Soil Mech. Found. Eng., Mexico, Vol. 4, pp. 225-290
13. Rowe, P. W.(1952), Anchored sheet pile walls, Proc., Institution of Civil Engineers, Vol. 1, Part 1, pp. 27-70
14. Terzaghi, K., and Peck, R. B.(1967), Soil mechanics in engineering practice, 2nd ed., John Wiley and Sons, Inc., New York, N. Y., 1967
15. Yang, G. S.(1996), Analysis of adjacent ground movements for deep excavations in urban areas, Ph.D. Dissertation, Seoul University

(received on Apr., 15. 1999)